Theoretical Analysis of Novel Wound-Field Synchronous Motor Self-Excited by Space Harmonics

Masahiro Aoyama[†], Toshihiko Noguchi **

*Shizuoka University, 3-5-1 Johoku, Naka-ku, Hamamatsu, Shizuoka 432-8561, Japan
[†]Suzuki Motor Corporation, 300 Takatsuka-cho, Minami-ku, Hamamatsu, Shizuoka 432-8611, Japan

Keywords: synchronous motor, self-excitation, space harmonics, concentrated winding, induced current.

Abstract

This paper describes a theoretical analysis of a self-excited wound-field synchronous motor in which space harmonics power is utilized for field magnetization instead of permanent magnets. The operation principle of the proposed motor can be explicated by a voltage equation on the synchronous rotating reference frame. The effect of an auxiliary pole designed to be magnetically independent of the main magnetic flux path and placed on the *q*-axis is mathematically discussed, and is analytically investigated through FEM based computer simulations.

1 Introduction

Recently, a various technical portfolios are considered, e.g., low-end hybrid system based on a 12 V idling stop system, and a high efficiency power train technology with high electrification ratio by using a rechargeable battery of several hundreds voltage, because of achieving a zero-emission. As an electric-machine energy conversion device, an Interior Permanent Magnet Synchronous Motor (IPMSM) is commonly applied to Hybrid Vehicles (HEVs) and Electric Vehicles (EVs) because of its high efficiency [1]. Permanent magnets used for the IPM motor are, however, very expensive because Nd-Fe-B magnets are generally employed to achieve higher energy density and to improve fuel efficiency at low-load operation for street use. Moreover, the traction motors are usually installed on the chassis, where special countermeasures must be taken from the viewpoints of environmental and thermal issues. In order to restrain demagnetization caused by temperature rise of the permanent magnets for example, expensive rare-earth metals such as Dy and Tb must be added to the Nd-Fe-B magnets. A material technology development, which is intensively placed Dy and Tb where the demagnetizing point easily, is actively engaged. However, a grobal maldistribution problem of the natural resources such as Dy and Tb is not discussed. The authors already proposed a rare-earth-free motor utilizing the space harmonics for the field magnetization power [2]. The purpose of the motor is to obtain a next position of the conventional IPMSM by achieving the comparable torque density with rare-earth-free permanent magnets. The proposed motor is a kind of the self-excited wound-field synchronous motors but is completely different from the recently proposed separated-excited wound-field machines, i.e., the wound-field flux switching motor and the brushless doubly salient motor [3][4]. The proposed motor can eliminate an external DC-coil on the primary side. The external DC-coil detrimentally affects the armature coil space factor and requires an additional auxiliary chopper circuit for the excitation. In addition, it is not necessary to supply a large field current in the DC field winding for the rotor magnetization. In the past works of the authors, however, qualitative discussion on the basis of the theoretical analysis has not been accomplished to explain the effect of the auxiliary pole, which is a special pole exclusively used for the magnetizing energy generation from the third space harmonics.

In this paper, a theoretical discussion of the effect of the auxiliary pole is conducted. It is mathematically and analytically explained in the discussion that the third space harmonics power can be mainly retrieved for the field magnetization power. Then, it is confirmed that the *d*-axis space harmonics magnetic path, where is aligned with rotor salient pole, organize a shorting magnetic path. It is mathematically and analytically discussed that placing the auxiliary pole on *q*-axis allows efficiently retrieving the field magnetization energy from the space harmonics is mathematically and analytically discussed. This placement of the auxiliary pole is also effective to increase the electromagnet torque.

2 Configuration and specifications of proposed motor

Figure 1 shows a cross section diagram of the proposed motor where the wound-field coils are installed to the rotor salient poles, and the induction coils are placed in spaces between the rotor salient poles, i.e., rotor slots. Conventional common motors such as a synchronous reluctance motor (SynRM) dissipate the space harmonics power caused by the stator with the concentrated winding structure, whereas the proposed motor positively takes advantage of the space harmonics power for the field magnetization. Each of the induction poles (I-pole) is a special pole exclusively used to generate the magnetizing power from the third space harmonics. In addition, it is magnetically independent of the main magnetic flux path to prevent reduction of the saliency ratio. The I-poles are held from an axial direction using a support ring as shown in Fig. 3. On the other hand, each

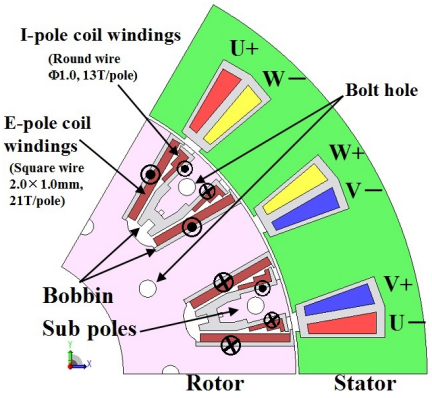

Fig. 1. Cross section diagram of proposed motor.

TABLE I SPECIFICATIONS OF MOTOR.

Number of poles	12
Number of slots	18
Stator outer diameter	200 mm
Rotor diameter	138.6 mm
Axial length of core	54 mm
Air gap length	0.7 mm
Maximum current	273 A_{pk} (60 s)
Stator winding resistance	32.1 mΩ / phase
Number of armature coil-turn	48
Number of I-pole coil-turn	13
Number of E-pole coil-turn	21
Winding connection	6 parallel
I-pole winding resistance	37.0 mΩ / pole
E-pole winding resistance	28.2 mΩ / pole
Thickness of iron core steel plate	0.35 mm

excitation pole (E-pole) has saliency on the rotor for the field excitation, which uses the retrieved third space harmonics power. Every I-pole and E-pole is connected in series via a diode rectifying circuit as shown in Fig. 2, where p indicates a pole number. Rotor windings are connected using a connection board on the rotor as shown in Fig.3, and the diode is fixed on a connection board by resin mold. Specifications of the motor are listed in Table I.

3 Theoretical analysis

3.1 Mathematical model on *dq*-reference frame

Figure 4 shows a developed salient pole model of the motor. As can be seen in the figure, the rotor salient pole is aligned with the *d*-axis, and the *q*-axis is supposed to be between the two salient poles. Assuming a combination between the rotor pole counts and the stator slot counts is 2 to 3, a U-phase self-inductance L_u can be given by

$$L_U(\theta) = L_{S0} + L_S \cos 2\theta \,, \tag{1}$$

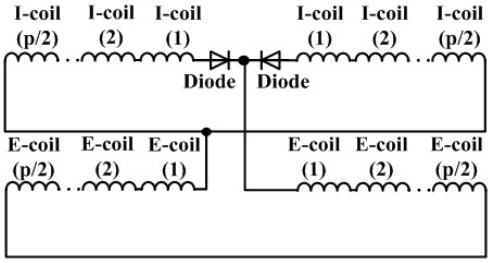

Fig. 2. Rotor winding connection diagram using full-bridge rectifier.

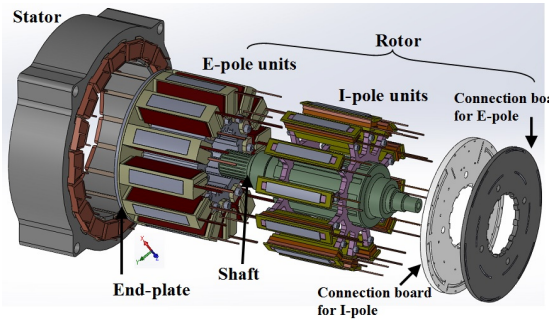

Fig. 3. Mechanical configuration of proposed motor.

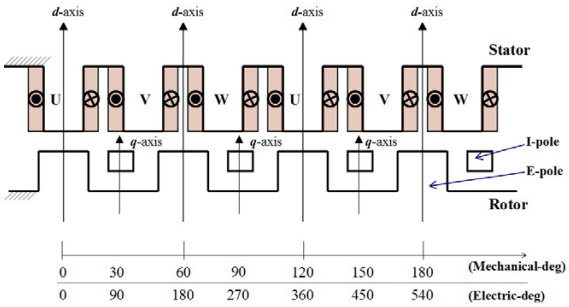

Fig. 4. Developed salient pole model of proposed motor.

where L_{S0} is a constant part and L_S is an amplitude of the periodical variation of the self inductance. Similarly, V-phase self inductance L_V and W-phase self inductance L_W can be given by

$$L_V(\theta) = L_{S0} + L_S \cos\left(2\theta - \frac{2}{3}\pi\right) \text{ and} \tag{2}$$

$$L_W(\theta) = L_{S0} + L_S \cos\left(2\theta + \frac{2}{3}\pi\right), \text{ respectively.} \tag{3}$$

An α-axis self inductance L_α and a β-axis self inductance L_β on the stationary orthogonal reference frame are obtained by a coordinate transform from three-phase to two-phase as follows:

$$L_\alpha(\theta) = L_U(\theta) + L_V(\theta)\cos\frac{2}{3}\pi + L_W \cos\frac{4}{3}\pi = \frac{3}{2}L_S \cos 2\theta \text{ and} \tag{4}$$

$$L_\beta(\theta) = L_V(\theta)\sin\frac{2}{3}\pi + L_W \sin\frac{4}{3}\pi = -\frac{3}{2}L_S \sin 2\theta \,. \tag{5}$$

Applying a rotational coordinate transform to the above equations by using a *d*-axis phase θ_d and a *q*-axis phase θ_q

expressed by Eq. (6), a d-axis self inductance L_d and a q-axis self inductance L_q can be obtained as Eqs. (7) and (8):

$$\theta_d = \omega t\,,\ \theta_q = \omega t - \frac{\pi}{2}\,, \tag{6}$$

$$L_d = \frac{3}{2} L_S \cos 2\omega t\ \text{, and} \tag{7}$$

$$L_q = \frac{3}{2} L_S \sin 2\omega t\,, \tag{8}$$

where ω is an electrical synchronous angular frequency.

Then, assuming that the U-phase armature current is given by

$$i_U(t) = I_S \cos(\omega t + \beta), \tag{9}$$

where β is a current phase, a magnetic flux of the U-phase $\varphi_{S\text{-}U}$ is derived as

$$\phi_{S-U} = \frac{L_U(\theta) i_U(t)}{N_S} = \frac{\{L_{S0} + L_S \cos 2\theta\} I_S \cos(\omega t + \beta)}{N_S}. \tag{10}$$

Other magnetic fluxes of the V-phase and the W-phase can be similarly derived as

$$\phi_{S-V} = \frac{\left\{L_{S0} + L_S \cos\left(2\theta - \frac{2}{3}\pi\right)\right\} I_S \cos\left(\omega t + \beta - \frac{2}{3}\pi\right)}{N_S}\ \text{, and} \tag{11}$$

$$\phi_{S-W} = \frac{\left\{L_{S0} + L_S \cos\left(2\theta + \frac{2}{3}\pi\right)\right\} I_S \cos\left(\omega t + \beta + \frac{2}{3}\pi\right)}{N_S}. \tag{12}$$

Therefore, the total three-phase armature flux is calculated as follows:

$$\begin{aligned}\phi_{S-UVW} &= \phi_{S-U} + \phi_{S-V} + \phi_{S-W} \\ &= \frac{3}{2}\frac{1}{N_S} L_S I_S \cos(\omega t + \beta - 2\theta)\cdot\end{aligned} \tag{13}$$

An α-axis magnetic flux $\varphi_{S\text{-}\alpha}$ and a β-axis magnetic flux $\varphi_{S\text{-}\beta}$ on the stationary orthogonal reference frame are obtained by the following rotational coordinate transform:

$$\begin{aligned}\phi_{S-\alpha} &= \phi_{S-U} + \phi_{S-V}\cos\frac{2}{3}\pi + \phi_{S-W}\cos\frac{4}{3}\pi \\ &= \frac{3}{2}\frac{I_S}{N_S}\left[L_{S0}\cos(\omega t + \beta) + \frac{1}{2} L_S \cos(\omega t + \beta + 2\theta)\right]\end{aligned}\ \text{, and} \tag{14}$$

$$\begin{aligned}\phi_{S-\beta} &= \phi_{S-V}\sin\frac{2}{3}\pi + \phi_{S-W}\sin\frac{4}{3}\pi \\ &= \frac{3}{2}\frac{I_S}{N_S}\left[L_{S0}\sin(\omega t + \beta) + \frac{1}{2} L_S \sin(\omega t + \beta + 2\theta)\right]\cdot\end{aligned} \tag{15}$$

Applying a rotational coordinate transform to the above equations by using the d-axis phase θ_d and the q-axis phase θ_q given by Eq. (6), the d-axis magnetic flux φ_d and the q-axis magnetic flux φ_q are obtained as below:

$$\phi_d = \frac{3}{2}\frac{I_S}{N_S}\left[L_{S0}\cos(\omega t + \beta) + \frac{1}{2} L_S \cos(3\omega t + \beta)\right]\ \text{, and} \tag{16}$$

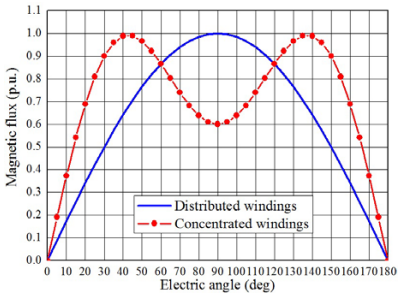

Fig. 5. Magnetic flux waveform.

$$\phi_q = \frac{3}{2}\frac{I_S}{N_S}\left[L_{S0}\sin(\omega t + \beta) + \frac{1}{2} L_S \sin(3\omega t + \beta)\right]. \tag{17}$$

Equations (16) and (17) indicate that the magnetic flux wave form does not have sinusoidal distribution but is distorted by the third space harmonics as shown in Fig. 5. In general, the magnetic flux density distribution of the distributed windings is sinusoidal but the magnetic flux density distribution of the concentrated windings is far from the sinusoidal waveform as mathematically indicated by Eqs. (16) and (17). Therefore, Eqs. (16) and (17) imply that the field magnetization energy for the self-excitation can be mainly obtained from the third space harmonics. Since the dq-reference frame rotates synchronously at the angular frequency ω, the rotor winding and the d-axis and the q-axis magnetic fluxes hold magnetic coupling of the higher frequency than the synchronous speed.

Then the mathematical model of the proposed motor can be obtained as follows [5]:

$$\begin{bmatrix} v_{sd} \\ v_{sq} \end{bmatrix} = \begin{bmatrix} R_s & 0 \\ 0 & R_s \end{bmatrix}\begin{bmatrix} i_{sd} \\ i_{sq} \end{bmatrix} + \begin{bmatrix} L_d & 0 & \frac{N_{rd}}{N_S}L_d & 0 \\ 0 & L_q & 0 & \frac{N_{rq}}{N_S}L_q \end{bmatrix} \mathrm{p} \begin{bmatrix} i_{sd} \\ i_{sq} \\ i_{rd} \\ i_{rq} \end{bmatrix}.$$
$$+\omega \begin{bmatrix} 0 & -L_q & -2\frac{N_{rd}}{N_S}L_q & -\frac{N_{rq}}{N_S}L_q \\ L_d & 0 & \frac{N_{rd}}{N_S}L_d & 2\frac{N_{rq}}{N_S}L_d \end{bmatrix} \begin{bmatrix} i_{sd} \\ i_{sq} \\ i_{rd} \\ i_{rq} \end{bmatrix} \tag{18}$$

The first term of the above equation is a voltage drop by the armature winding resistance, the second term is a transformer electromotive force, and the third term corresponds to a velocity electromotive force. Furthermore, the output torque of the proposed motor is obtained by the vector product between the armature current and the magnetic flux which is described as a part of the third term of Eq. (18). The output torque is expressed as

$$\begin{aligned} T &= P_p \begin{bmatrix} i_{sd} & i_{sq} \end{bmatrix} \begin{bmatrix} 0 & -L_q & -2\frac{N_{rd}}{N_S}L_q & -\frac{N_{rq}}{N_S}L_q \\ L_d & 0 & \frac{N_{rd}}{N_S}L_d & 2\frac{N_{rq}}{N_S}L_d \end{bmatrix} \begin{bmatrix} i_{sd} \\ i_{sq} \\ i_{rd} \\ i_{rq} \end{bmatrix}, \\ &= P_p (L_d - L_q) i_{sd} i_{sq} \\ &\quad + \frac{P_p}{N_S}\{N_{rd}(L_d i_{sq} - 2L_q i_{sd}) i_{rd} - N_{rq}(L_q i_{sd} - 2L_d i_{sq}) i_{rq}\} \end{aligned} \tag{19}$$

where P_p is a pole-pair number. As expressed in the above equation, the output torque consists of two terms, i.e., reluctance torque and electromagnet torque [5]. The former is basically independent of the operation angular frequency ω. Here, it is possible to rewrite i_{rd} and i_{rq} with i_{sd} and i_{sq} because i_{rq} is induced through the mutual inductance between the stator and the rotor. It should be noted that the third space harmonics caused by the stator concentrated winding structure are superimposed on i_{rq} through the induction process. The induced voltage of the I-pole windings, which includes the third space harmonics component, can be obtained as

$$\begin{aligned} v_{rq} &= -N_{rq}\mathrm{p}\begin{pmatrix} K_{d-axis}\dfrac{3}{4}\dfrac{L_S I_S}{N_S}\cos(3\omega t+\beta) \\ +K_{q-axis}\dfrac{3}{4}\dfrac{L_S I_S}{N_S}\sin(3\omega t+\beta)\end{pmatrix}, \\ &= \frac{9\omega}{4}\frac{N_{rq}}{N_S}L_S I_S\begin{Bmatrix} K_{d-axis}\sin(3\omega t+\beta) \\ -K_{q-axis}\cos(3\omega t+\beta)\end{Bmatrix} \end{aligned} \quad (20)$$

where $K_{d\text{-}axis}$ and $K_{q\text{-}axis}$ are leakage magnetic flux coefficients and their values range from 0 to 1. Thus, the voltage applied to E-pole winding is expressed by Fourier series and a developed formula of Fourier series on an absolute value of Eq. (20). In addition, simplify a calculation with ignoring a time function terms, the voltage applied to E-pole winding can be given by

$$\begin{aligned} v_{rd(DC)} &= \frac{9\omega}{2\pi}\frac{N_{rq}}{N_S}L_S I_S\left(K_{d-axis}\cos\beta + K_{q-axis}\sin\beta\right) \\ &= \frac{9\omega}{2\pi}\frac{N_{rq}}{N_S}L_S\left(K_{d-axis}i_{sd}+K_{q-axis}i_{sq}\right) \end{aligned}. \quad (21)$$

Then, a field current i_{rd} flows through the voltage by applying to an E-pole winding. The field current is given by solving the transitional phenomenon of a rotor winding expressed with R-L equivalent circuit, and i_{rd} can be obtained as

$$i_{rd}(t) = \frac{v_{rd(DC)}}{R_{rq}+R_{rd}}\left(1-e^{\frac{-(R_{rq}+R_{rd})}{L_{rd}}t}\right). \quad (22)$$

As shown in Fig. (2), induced current in I-pole winding becomes the value that a half-bridge rectified of field current in E-pole windings. Considering a leakage inductance to approximate an actual mutual inductance, the torque equation of Eq. (19) is rewritten as

$$\begin{aligned} T &= P_p\left(L_d - L_q\right)i_{sd}i_{sq} \\ &+ P_p\frac{N_{rq}}{N_S^2}\frac{K_S L_S}{R_{rd}+R_{rq}}\frac{9\omega}{2\pi}\left(K_{d-axis}i_{sd}+K_{q-axis}i_{sq}\right)* \\ &*\begin{Bmatrix} -K_{Lq}L_q\left(2N_{rd}+\dfrac{N_{rq}}{\pi}\right)i_{sd} \\ +K_{Ld}L_d\left(N_{rd}+\dfrac{2N_{rq}}{\pi}\right)i_{sq}\end{Bmatrix} \end{aligned}, \quad (23)$$

where K_S, K_{Ld} and K_{Lq} are leakage magnetic flux coefficients. The coefficients have values ranging from 0 to 1.

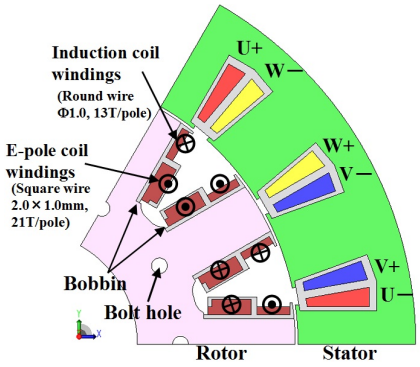

Fig. 6. Model without auxiliary poles.

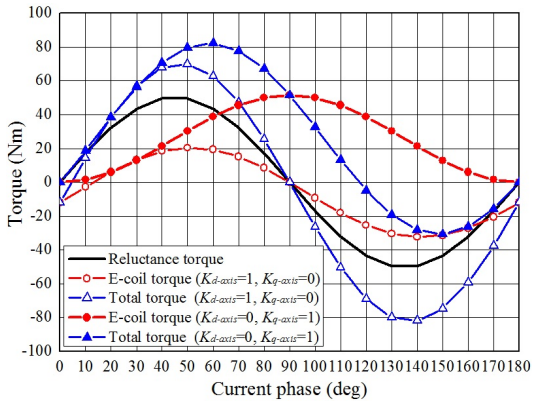

Fig. 7. Current phase-torque characteristics calculated by mathematical model (average torque in steady state).

3.2 Effect of auxiliary poles on q-axis

Figure 6 shows a motor cross section diagram with wound-field coils on the rotor salient poles. The induction coils are aligned with the d-axis instead of q-axis between the two salient poles. The specifications of the model without the auxiliary poles have not been changed except for the I-coil winding placement. Both of the two models shown in Figs. 1 and 6 can be mathematically represented by adjusting $K_{d\text{-}axis}$ and $K_{q\text{-}axis}$. Setting $K_{d\text{-}axis}$ =0 corresponds to the model with the auxiliary poles on the q-axis, while $K_{q\text{-}axis}$ =0 represents the model with no auxiliary poles on the q-axis. A cross-linkage magnetic flux between the d-axis and the q-axis is ignored for simplification of the calculation. Figure 7 shows calculation results in the cases of $K_{d\text{-}axis}$ =0 and $K_{q\text{-}axis}$ =0 given by Eq. (23). The effect on saliency caused by the auxiliary pole is ignored. As shown in Fig. 7, mounting the auxiliary poles on the q-axis has significant effect to enlargement of the output torque. It can be found that harmonic magnetic flux on the q-axis plays the most important role to increase the electromagnetic torque. In addition, the q-axis is considered to be the induction poles for the field magnetization because the d-axis is aligned with the salient electromagnet poles.

Then, the theory of setting the I-pole on q-axis can be explicated below by FEM analysis results. Figure 8 shows a magnetic flux vectors and flux lines of the third space harmonics simulated by the magnetic field analysis. As shown in the figure, the third space harmonics magnetic flux

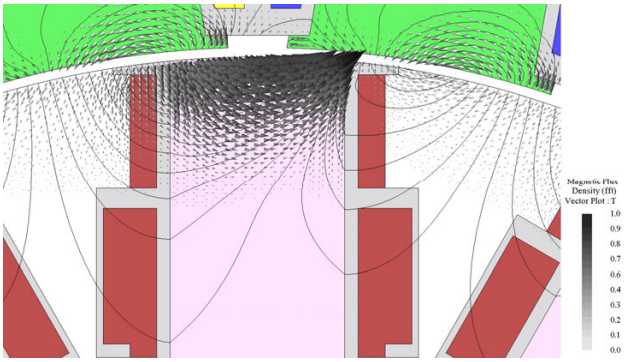

(a) Without auxiliary poles.

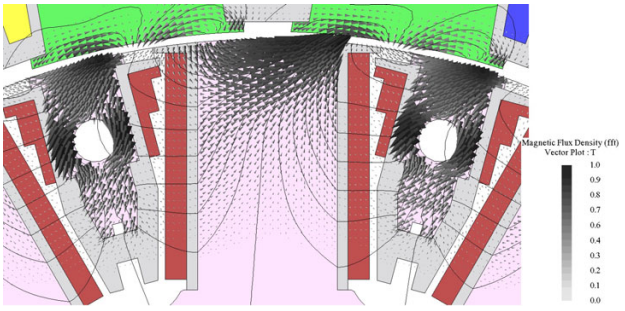

(b) With auxiliary poles (proposed model).

Fig. 8. Third space harmonics vector and flux lines.

mainly flows through a space between the rotor salient poles, of which direction corresponds to the *q*-axis, and leaks to the salient poles on the *d*-axis. Therefore, the third space harmonics power can efficiently be retrieved by placing auxiliary poles on the *q*-axis as shown in Fig. 8 (b). Since the model without auxiliary poles has both of the induction coil and the excitation coil on the same salient pole, which is the *d*-axis, it is rather difficult to retrieve the third space harmonics power efficiently. The rotor tooth width widely is required to prevent magnetic saturation, because the salient pole, which is wound the E-pole winding, is magnetized by field current. However, the expansion of its width negatively effects the organization of shorting magnetic path of third space harmonics as shown in Fig. 8 (a). The model with auxiliary poles shown in Fig. 8 (b), however, has the induction coil and the excitation coil separately on the *q*-axis and the *d*-axis, respectively, which results in effective retrieval of the third space harmonics power. As shown in Fig. 8 (b), it is confirmed the third space harmonics magnetic flux is orthogonal to an I-pole.

4 FEM analysis

Figure 9 shows current phase-torque (average torque in steady state) characteristics at 1000 r/min of the model without auxiliary poles and with auxiliary poles simulated by FEM based computer simulations. As shown in Fig. 9, the electromagnet torque (E-coil torque), i.e., an additional torque generated by the self-excitation using the space harmonics, is enlarged by setting the auxiliary poles on the *q*-axis. Figure 10 shows induced current under MTPA (Max Torque Per

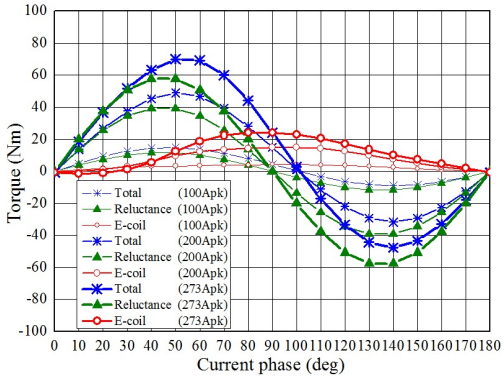

(a) Without auxiliary poles.

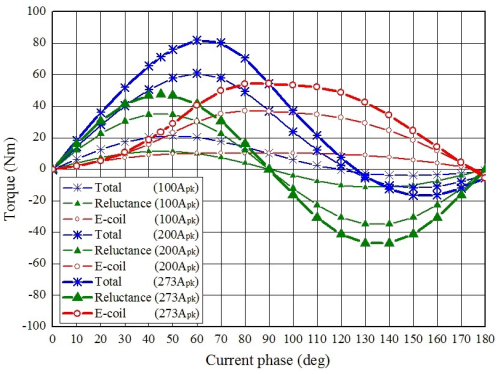

(b) With auxiliary poles (proposed model).

Fig. 9. Current phase-torque characteristics at 1000 r/min simulated by FEM model (average torque in steady state).

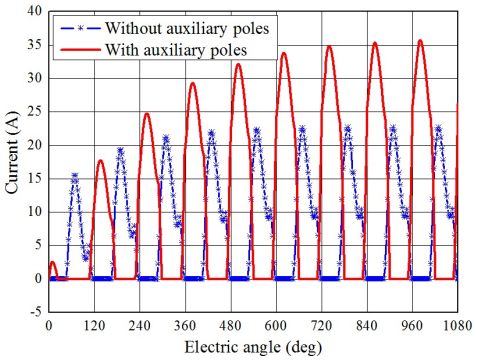

Fig. 10. Induced current of I-pole windings in forward direction.

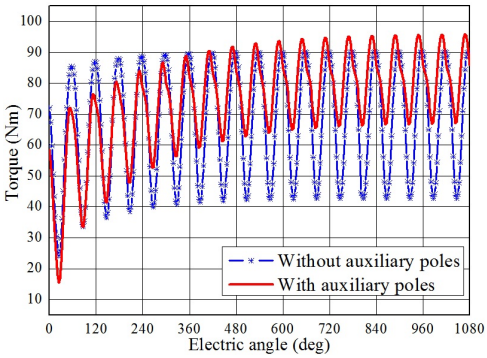

Fig. 11. Torque characteristics at 1000 r/min under MTPA control.

Ampere) control of the series connected I-pole windings in forward direction of the diode rectifying circuit. As can be seen in the figure, the induced current of the model with auxiliary poles is much higher than that of the model without auxiliary poles, which demonstrates effectiveness of the optimum placement design of the auxiliary poles. Figure 11 shows the torque characteristics at 1000 r/min and 273 A_{pk} under MTPA control calculated by the magnetic field analysis. As shown in the figure, placing the auxiliary poles greatly contributes to increase the output torque. Moreover, another superior point of the proposed model can be found in the torque ripple characteristic. The torque ripple of proposed model is 37.8 % under MTPA control, which is remarkably improved from the model without auxiliary model (68.6 %). Figure 12 shows adjustable speed drive characteristics of the model without auxiliary poles and with it. As indicated by Eq. (23), the higher electromagnet torque is delivered as the synchronous speed increases because the self-excited E-coil torque is proportional to the speed. As the most important point, the model with auxiliary poles can be dramatically increase the total output torque by the exclusive poles greatly contributes to increase the electromagnet torque. In addition, it can be confirmed that it is essential to feed the induced current from the I-pole windings, due to increase the total output torque. The current phase control (general vector control) can be accommodated the induced voltage on the terminal to satisfy the voltage limit at the terminal, and the model with auxiliary poles can be dramatically increase the output toque as proportional to the rotating speed.

5 Conclusion

This paper has theoretically and analytically discussed the effect of the auxiliary poles placed on the *q*-axis. It has been clarified through the mathematical analysis that the effect of auxiliary poles, which is a special pole exclusively used for the magnetizing power generation from the third space harmonics. In addition, the advantages, which the wound-field coils are added to the rotor salient poles and the induction coils are placed in spaces between the rotor salient poles, is analytically cleared by confirming a magnetic flux vector and flux lines of the third space harmonics simulated by FEM. Furthermore, the current phase-torque characteristics have been clarified by the FEM based computer simulation. The electromagnet torque caused by the third space harmonics and the reluctance torque caused by the saliency are simultaneously generated in the proposed motor, but the electromagnet torque generated by the I-poles and E-poles on the rotor takes significant part of the total torque. That additional torque can be increased by placing the I-poles on the *q*-axis, where *q*-axis harmonic magnetic flux can be retrieve effectively. The future work of the study is to set up an actual prototype machine to verify the theoretical discussion and the analysis results through experimental tests. It is also important to develop the mathematical model since estimation of the induced current and the field current of the rotor windings is significantly important for the proposed motor.

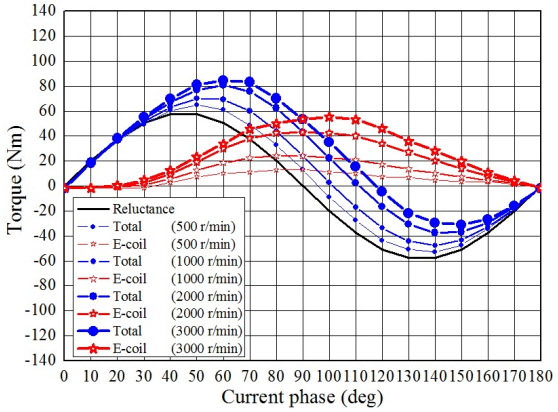

(a) Without auxiliary poles.

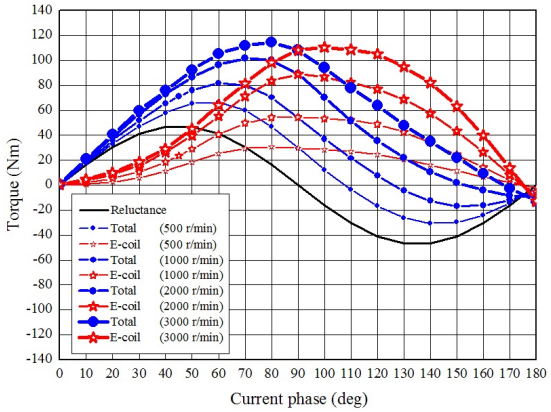

(b) With auxiliary poles (proposed model).

Fig. 12. Adjustable speed drive characteristics at maximum load (average torque in steady state).

References

[1] Y. Sato, S. Ishikawa, T. Okubo, M. Abe and K. Tamai, "Development of High Response Motor and Inverter System for the Nissan LEAF Electric Vehicle," SAE Technical Paper 2011-01-0350. 2011, doi:10.4271/2011-01-0350.

[2] M. Aoyama, T. Noguchi, "Rare-Earth Free Motor with Field Poles Excited by Space Harmonics," ICRERA'13 *Proc.*,ID:69, Oct., 2013.

[3] C. Pollock, H. Pollock, R. Barron, J.R. Coles, D. Moule, A. Court and R. Sutton, "Flux-Switching Motors for Automotive Applications," *IEEE Trans.* I.A., Sep./Oct. 2006, vol.42, no.5, pp.1177-1184.

[4] L. Sun, Z. Zhang and L. Qian, "Calculation and Analysis of Iron Loss in Doubly Salient Brushless DC Generator," IECON'13 *Proc.*, pp.2648-2651, Nov. 2013.

[5] M. Aoyama, T. Noguchi, "Improved Mathematical Model of Wound-Field Synchronous Motor Self-Excited by Space Harmonics," *IEE-Japan Technical Meeting*, SPC-14-007/MD-14-007 (2014, in Japanese).